ACS Sustainable Chemistry & Engineering

Research Article

pubs.acs.org/journal/ascecg

Three-Dimensional Flower-Shaped Activated Porous Carbon/Sulfur Composites as Cathode Materials for Lithium−Sulfur Batteries

Lan Zhou, Tao Huang,* and Aishui Yu*

Department of Chemistry, Shanghai Key Laboratory of Molecular Catalysis and Innovative Materials, Institute of New Energy, Fudan University, Shanghai 200438, China

ABSTRACT: In this study, three-dimensional flower-shaped activated porous carbon/sulfur composites (FA-PC/S) are fabricated for the first time via a simple method utilizing flower-shaped ZnO as a template and pitch as the carbon precursor, followed by carbonization activation and thermal treatment. The composites are characterized using scanning electron microscopy (SEM), transmission electron microscopy (TEM), Brunauer−Emmett−Teller (BET) analysis, Raman spectroscopy, X-ray powder diffraction (XRD), and thermogravimetric (TG) measurements. The results show that sulfur is well dispersed and encapsulated homogeneously in the micropores of the flower-shaped activated porous carbon (FA-PC) with excellent electrical conductivity, high surface area, and large pore volume. The electrochemical tests show that the FA-PC/S composites with 60 wt % S have a high initial discharge capacity of 1388 mA h g^{-1} at 100 mA g^{-1}, good cycling stability (reversible discharging capacity of approximately 600 mA h g^{-1} at 1600 mA g^{-1}), and excellent rate capability.

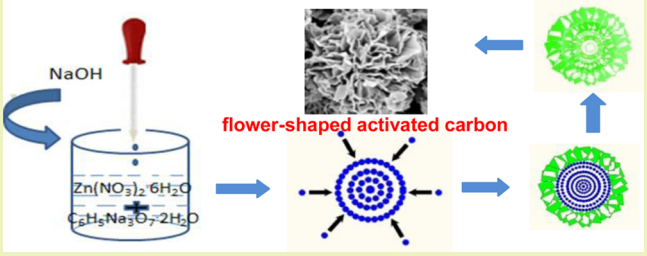

KEYWORDS: *Flower-shaped activated porous carbon, Micropores, Lithium−sulfur cell, Cathode material*

INTRODUCTION

Along with the development of energy shortages and global environmental problems, new electrode materials for Li-ion batteries have been receiving increased attention because of their unique electrical and chemical properties for applications in portable electronic devices. In particular, elemental sulfur has been extensively investigated as a promising cathode material for lithium−sulfur batteries because of its high theoretical specific capacity of 1675 mA h g^{-1}, high theoretical specific energy of 2600 W h kg^{-1}, abundant sources, low cost, nontoxicity, and environmental friendliness.[1−6] However, some troublesome issues associated with sulfur cathodes severely limit the utilization of sulfur in electrodes and the electrochemical performance of lithium−sulfur batteries. For instance, the high solubility of lithium polysulfide intermediates in organic electrolytes from the electrochemical reduction process[7−9] results in a shuttle effect of dissolved polysulfide ions between the sulfur cathode and the lithium anode, which eventually leads to a deposition of insoluble and insulating Li_2S_2/Li_2S on the electrode surface, a drastic reduction in the specific capacity, and a fast decline in the capacity.[10,11] Additionally, both the high insulating ability and volume expansion of sulfur will reduce the electrode conductivity and cause deterioration of the cathode integrity. To overcome these issues and improve the specific capacity and cycling performance of lithium−sulfur batteries, various types of carbon materials have been extensively applied to sulfur composite cathodes in recent years,[12−19] such as carbon nanotubes/nanofibers, mesoporous carbon, graphene, hollow carbon, microporous carbon, hierarchical porous carbon, and carbon spheres. Notably, recent results suggest that different types of carbon materials with good conductivity, high surface area, and large pore volume have been regarded as the ideal matrix for sulfur to improve the cycling performance and the rate capability of lithium−sulfur batteries.

In our work, three-dimensional flower-shaped activated porous carbon/sulfur composites (FA-PC/S) for lithium−sulfur batteries have been prepared for the first time using a simple method using flower-shaped ZnO as a template, pitch as the carbon precursor, and KOH as an activating agent, followed by carbonization activation and thermal treatment.[20−24] A typical flower-shaped FA-PC spherical structure is composed of many nanopetals intersecting one another. The process of how the flower-shaped 3D activated porous carbon structures were formed is illustrated in Scheme1. Because of the unique three-dimensional flower-shaped porous spherical structure, FA-PC has high reactivity, high electrical conductivity, and a short transport length for the Li ion. Furthermore, the rich micropores of the FA-PC offer enough space to accommodate the volume expansion that occurs during the discharge process of the encapsulated sulfur as well as confine the electrochemical reaction products of the sulfur cathode within the micropores; thus, the FA-PC/S cathode material exhibits excellent electrochemical properties.[25]

Received: July 17, 2014
Revised: September 3, 2014
Published: September 19, 2014

   dx.doi.org/10.1021/sc500459c | *ACS Sustainable Chem. Eng.* 2014, 2, 2442−2447

Scheme 1. Illustration of Preparation of FA-PC Material

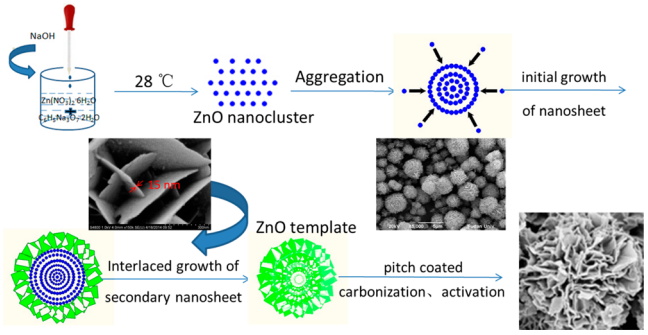

EXPERIMENTAL SECTION

Preparation of Flower-Shaped Activated Porous Carbon (FA-PC) and Flower-Shaped Activated Porous Carbon/Sulfur (FA-PC/S). In a typical experiment, the flower-shaped 3D ZnO template was obtained as follows:[20−22] 1.48 g of $Zn(NO_3)_2{\cdot}6H_2O$ and 3.52 g of $HOC(COONa)(CH_2COONa)_2{\cdot}2H_2O$ were completely dissolved in 100 mL of deionized water under stirring. Then, 1 g of NaOH was dissolved in 20 mL of water and gradually added to the above solution. Afterward, a white precipitate of flower-shaped 3D ZnO was produced after continuously stirring for 2 h at 28 °C. Finally, the as-prepared ZnO was collected by centrifugation, washed thoroughly with deionized water to remove the residues, and dried under vacuum at 100 °C. To prepare the flower-shaped activated porous carbon (PC), 0.40 g of as-prepared flower-shaped 3D ZnO as a template and 0.10 g of pitch as a carbon precursor were dispersed in 60 and 20 mL of THF solvent, respectively. After violently stirring for 1 h, the 20 mL pitch dispersion was gradually added to the 60 mL ZnO solution. The mixture was stirred for 6 h and then dried at 60 °C, and the resulting solid was heated to 500 °C under N_2 atmosphere and maintained for 2 h. The obtained powder was further dispersed in distilled water, followed by washing with an aqueous solution of HCl to remove the ZnO template until the filtrate was neutral. The product of PC was gathered and dried at 100 °C for 12 h in a vacuum oven. The resulting PC material and KOH (at a 1:2 mass ratio) were dissolved in 40 mL of aqueous solution, stirred for 1 h at room temperature, and then dried at 100 °C to thoroughly remove the solvent. The resulting mixture was carbonized at 850 °C for 2 h under N_2 atmosphere. Finally, the acquired product was treated with an aqueous solution of HCl and washed repeatedly with deionized water to remove the residual potassium hydroxide until the filtrate was neutral. After collecting and drying at 100 °C for 12 h, the FA-PC material was successfully prepared.

The prepared FA-PC material (0.04 g) and sublimed sulfur (0.06 g) were mixed and ground for 1 h in a quartz mortar and then sealed in a PTFE container full of N_2 atmosphere. The PTFE container was first heated to 155 °C and maintained for 24 h and then thermally treated at 160 °C for 12 h to further guarantee that the melting sulfur could diffuse into the abundant micropores of the FA-PC.[26,27] Finally, the obtained composite was named FA-PC/S. For comparison, a PC/S composite was prepared by using the same sulfur−carbon ratio and thermal treatment as mentioned above.

Morphological Characterization and Electrochemical Measurements. The synthesized composite was characterized by powder X-ray diffraction (Bruker D8 Advance, Cu Kα radiation = 1.5406 Å) and Raman microscopy (Renishaw, U.K.), and nitrogen adsorption isotherms were determined using a Quantachrome Autosorb-1-MP instrument (77 K, Quantachrome, U.S.A.). The flower-shaped structures of the composite were studied by field-emission scanning electron microscopy (FE-SEM, Hitachi S-4800) and transmission electron microscopy (TEM, JEOL-2100F, Japan). Thermogravimetric (TG) measurements were conducted to measure the weight content of sulfur in the composites on a Mettler Toledo TGA-SDTA851 instrument under N_2 atmosphere (500 °C, 10 °C min^{-1}). The FA-PC/S and PC/S electrodes were prepared from a mixture of carbon/sulfur composites, Super P, and PVDF binder (70:15:15) in a *N*-methyl-2-pyrrolidone (NMP) dispersant. The slurry was uniformly cast onto carbon-coated Al foil by a doctor blade. After the solvent volatilized, the cathode was cut into disks (d = 12 mm), which were subsequently dried at 60 °C for 18 h in a vacuum oven. The half-cells with Li as the counter electrode and a Celgard 2300 sheet as a separator were assembled in an argon-filled glovebox (Mikarouna, Superstar 1220/750/900) and tested with a LAND instrument (CT2001A, Wuhan Jinnuo Electronic Co., Ltd.). The electrolyte utilized was 3 M LiTFSI in a solution of 1,3-dioxolane (DOL)/1,2-dimethoxyethane (DME) (2:1 by volume). The mass of the electrode material is about 2 mg, and the electrode surface area is 1.13 cm^2 (Φ = 12 mm). The specific capacity values in this paper were calculated on the basis of the active sulfur mass in the charge−discharge measurements.

RESULTS AND DISCUSSION

Morphology and Structure of FA-PC and FA-PC/S Composites. FESEM and TEM images were used to confirm the morphologies of the flower-shaped 3D FA-PC and FA-PC/S composites. The FESEM images in Figure 1a and b and TEM image in Figure 2a show that the as-synthesized PC material exhibits a uniform flower-shaped structure, which is built from numerous intersecting nanopetals, and the thickness of the carbon nanoflakes is approximately 15 nm. After KOH treatment, the FA-PC retains its flower-shaped morphology, but an obvious curling of the carbon nanoflakes and interconnected network of macropores can be observed, as shown in Figure 1c and d and Figure 2b, indicating that a portion of the carbon was corroded in the chemical activation process leading to the production of abundant micropores. After the active sulfur impregnation, both the FESEM images (Figure 1e,f) and TEM images (Figure 2c) of the FA-PC/S composite demonstrate a flower-shaped 3D superstructure similar to the original FA-PC material. No obvious surface

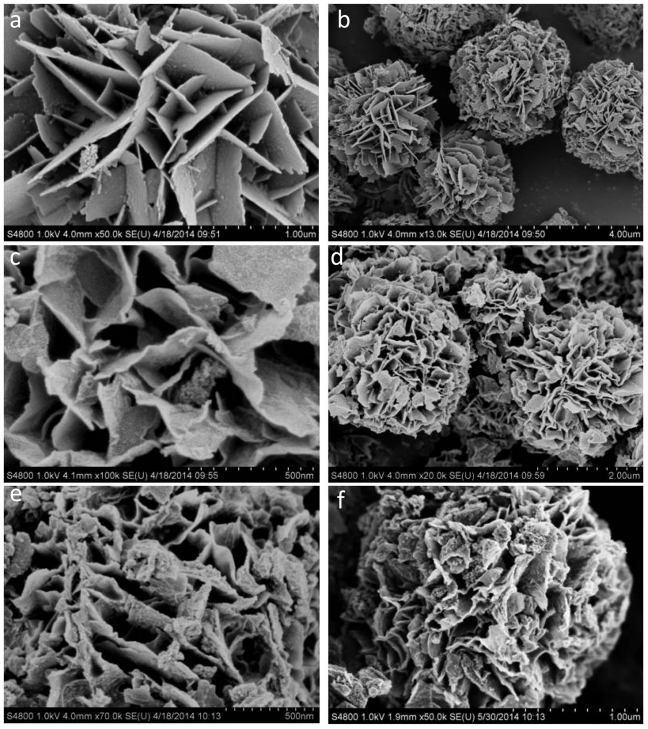

Figure 1. FESEM images of PC (a,b), FA-PC (c,d), and FA-PC/S (e,f) at high magnification.

dx.doi.org/10.1021/sc500459c | ACS Sustainable Chem. Eng. 2014, 2, 2442−2447

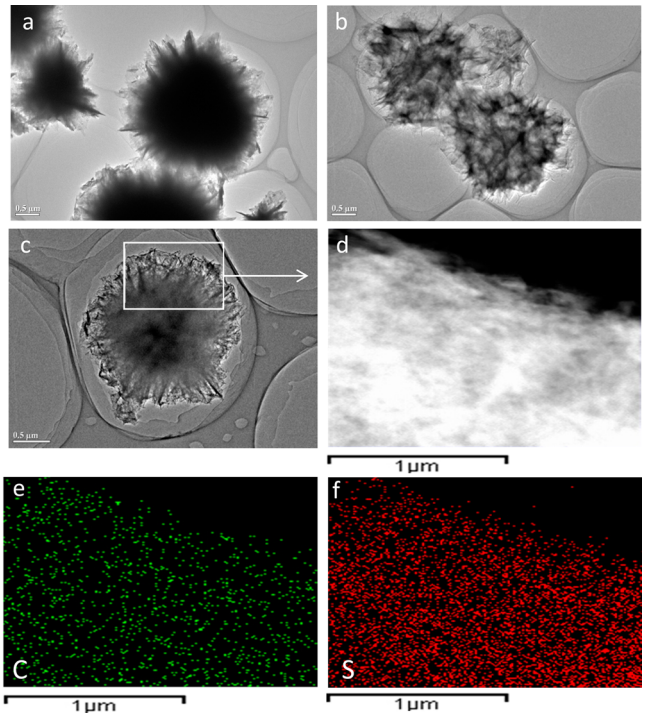

Figure 2. TEM images of PC (a), FA-PC (b), and FA-PC/S (c) at high magnification and the corresponding element mapping of C/S (d–f).

deposition or aggregation of active sulfur inside or outside the flower-shaped 3D superstructure can be observed. The entrance of sulfur into the micropores of FA-PC was also investigated by elemental mapping at high magnification (Figure 2d–f). Both C and S elements were found to be uniformly distributed in the micropores of the FA-PC material, which was further confirmed by Brunauer–Emmett–Teller (BET) measurements. The pore structure of the FA-PC, PC, FA-PC/S, and PC/S composites were characterized by BET measurements (Figure 3a,b). A narrow pore size distribution determined by the density functional theory method determined the characteristic microporous superstructure of the FA-PC. Moreover, the large specific surface area of 2539 $m^2\ g^{-1}$ and the Vt of 1.48 $cm^3\ g^{-1}$ for the FA-PC composite offers an excellent opportunity for sulfur encapsulation. However, for the PC, although it has a similar pore structure as FA-PC, it is obvious that both the specific surface area of 1117 $m^2\ g^{-1}$ and the Vt of 1.16 $cm^3\ g^{-1}$ are lower than those of FA-PC, which further confirms that a portion of the carbon in the PC material was consumed upon KOH activation, resulting in the production of more micropores in the FA-PC material. After the sulfur was introduced in both PC and FA-PC, the specific surface areas were rapidly reduced to below 50 $m^2\ g^{-1}$. The homogeneous dispersion of sulfur in the micropores of FA-PC can also be explained by the X-ray diffraction patterns and Raman spectroscopy. The XRD results for the PC, FA-PC, S, PC/S, and FA-PC/S composites are shown in Figure 4a. The PC and FA-PC exhibit wide-angle XRD patterns with two broad characteristic diffraction peaks located at approximately 25° and 43°, which are ascribed to the (002) and (101) planes of graphite, respectively. Sublimed S exhibits several sharp crystal diffraction peaks, indicating that elemental sulfur typically exists in a crystalline state. After heating the mixture of sulfur and carbon, it is obvious that almost all of the characteristic diffraction peaks of sulfur appear

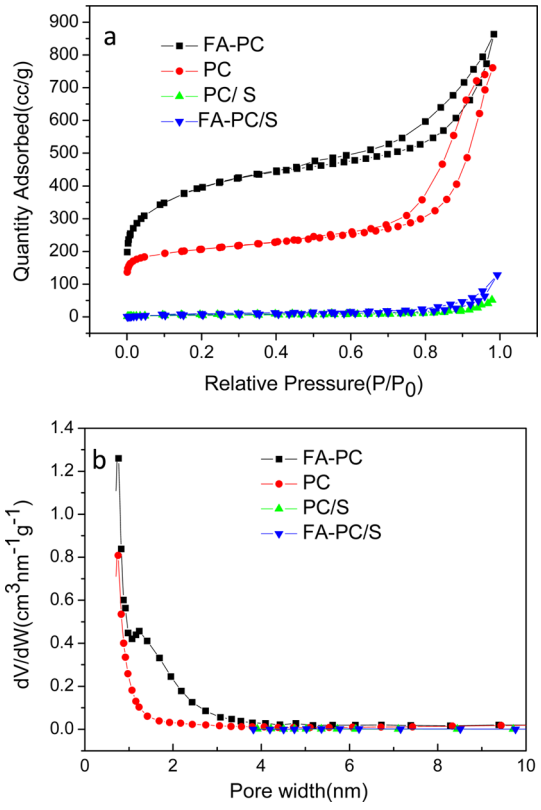

Figure 3. (a) Gas (N_2) adsorption–desorption isotherm loops. (b) BJH pore size distributions of PC, FA-PC, PC/S, and FA-PC/S.

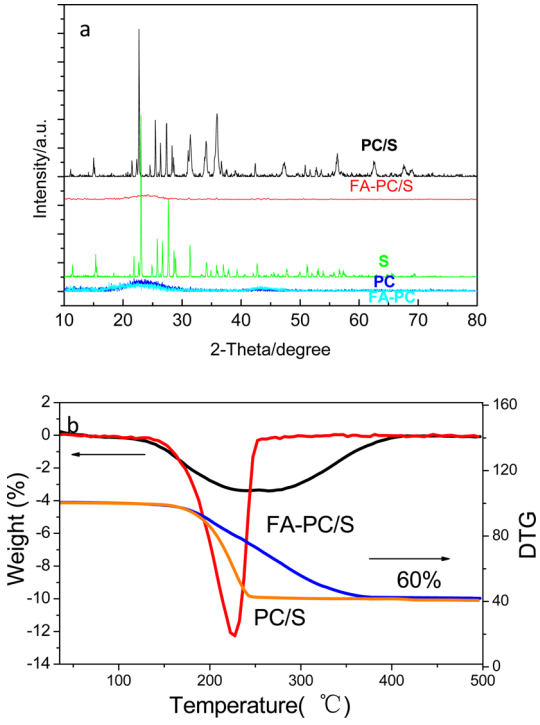

Figure 4. (a) XRD patterns of the PC, FA-PC, PC/S, and FA-PC/S composites. (b) TGA and DTG curves of the PC/S and FA-PC/S composites.

in the PC/S composite but entirely disappear in the FA-PC/S composite, demonstrating that sulfur is amorphous and uniformly distributed in the micropores of the FA-PC, which

dx.doi.org/10.1021/sc500459c | ACS Sustainable Chem. Eng. 2014, 2, 2442–2447

is consistent with the FESEM and TEM results. The 60 wt % sulfur content in the PC/S and FA-PC/S composited were measured by TGA, as shown in Figure 4b. Compared to those of the PC/S composite, the DTG curves of the FA-PC/S composite reflect a broader temperature range during the entire sulfur loss process. This observation may be attributed to the confinement of sulfur in the micropores of the FA-PC.

Electrochemical Performance of FA-PC/S Composites. Galvanostatic charging−discharging performance and rate capability evaluations were performed to investigate the electrochemical performance of the composite materials. Figure 5 shows the long cycling performance of FA-PC/S and PC/S at

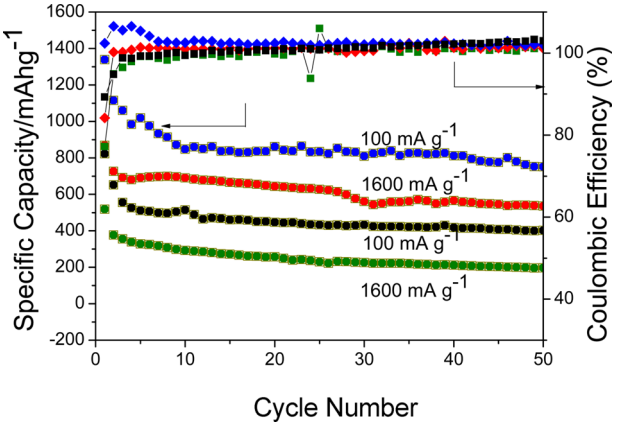

Figure 5. Cyclic performance and coulombic efficiency of FA-PC/S (red and blue, respectively) and PC/S (black and olive, respectively) electrodes at 100 mA g^{-1} and 1600 mA g^{-1}, respectively.

different current densities. For the FA-PC/S composite, a high initial discharge capacity of 1388 mA h g^{-1} at a current density of 100 mA g^{-1} was achieved, and the FA-PC/S electrode demonstrated good cycling stability with a reversible capacity of approximately 800 mA h g^{-1} after 50 cycles. However, for the PC/S electrode, a lower first discharge capacity of 822 mA h g^{-1} and reversible capacity of 400 mA h g^{-1} after 50 cycles with a current density of 100 mA g^{-1} were obtained. When increased to a higher current density of 1600 mA g^{-1}, an initial discharge capacity of 870 mA h g^{-1} was measured, and a reversible capacity of approximately 600 mA h g^{-1} was obtained after 50 cycles for the FA-PC/S electrode. In contrast, not only was a smaller initial discharge capacity of 520 mA h g^{-1} obtained but the discharge capacity was rapidly reduced to 200 mA h g^{-1} after 50 cycles for the PC/S electrode. Furthermore, for the FA-PC/S electrode, the coulomb efficiency was nearly 100% in addition to the first lap in the entire cycle, and the PC/S electrode showed the same result except for occasional fluctuations. The high coulomb efficiency indicated that the above electrodes can work well in the high concentration ether electrolyte without the addition of $LiNO_3$.[28−30] The reduced amount of overcharge can be attributed to an decrease in the polysulfide solubility in the high concentration organic electrolyte, which inhibited the shuttle effect in some degree.

The flower-shaped 3D FA-PC/S electrode also exhibited superior high-rate performance. A progressive rate-step test for the cells was implemented, as shown in Figure 6. The reversible capacity at a current density of 200 mA g^{-1} was approximately 820 mA h g^{-1} after 10 cycles. Subsequently, the reversible capacity decreased slowly with an increase in current density. When measured at a higher current density of 1600 mA g^{-1}, the

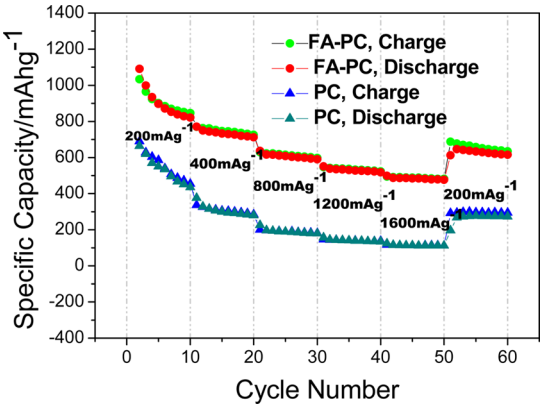

Figure 6. Discharge capacity of the FA-PC/S and PC/S electrodes at different rates.

specific capacity remained at approximately 500 mA h g^{-1} and could be recovered to approximately 700 mA h g^{-1} when the current density was reduced back to 200 mA g^{-1}. However, for the PC/S electrode, lower reversible capacity and faster attenuation of capacity with an increase in current density were clearly observed. The second, third, sixth, and tenth galvanostatic charge−discharge profiles at a current density of 200 mA g^{-1} are shown in Figure 7. For the FA-PC/S composite, two plateaus centered at ∼2.1 and ∼2.3 V were observed in the discharge profile, corresponding to the two typical characteristic plateaus of sulfur−carbon cathodes for lithium−sulfur batteries.[31−33] As reported in previous works, the upper plateau (∼2.3 V) results from the ring opening of S_8 upon reduction to linear high order lithium polysulfides (Li_2S_n, $n \geq 4$). The lower plateau (∼2.1 V) corresponds to the high-order lithium polysulfides transforming into low-order lithium polysulfides (Li_2S_n, $n < 4$).[34,35] The reversible capacity of 977 mA h g^{-1} was obtained in the second cycle at 200 mA g^{-1}, and the attenuation of specific capacity decreased as the number of cycles increased. However, for the PC/S electrode, there was a higher charging platform at 2.35 V. Furthermore, compared to the FA-PC/S electrode, a lower reversible capacity of 664 mA h g^{-1} in the second cycle at 200 mA g^{-1} and a faster capacity attenuation with an increasing number of cycles were obtained. The relatively superior cycle and rate capability of the FA-PC/S electrode may be attributed to its large surface area and high pore volume, which offer sufficient space to confine the occurrence of electrochemical reactions in the abundant micropores. This capability would not only effectively prevent active sulfur and intermediate products from dissolving in the electrolyte but also ensure the stability of the FA-PC/S material and the integrity of the electrode. Moreover, the macropores of stable flower-shaped 3D FA-PC/S composed of carbon sheets as ion-buffering reservoirs could offer a short diffusion distance, shorten the transport length for the Li ion, and facilitate the rapid transport of electrolyte ions to the interior of the material, which would further enhance its reactivity and electrical conductivity.[36,37]

CONCLUSIONS

In summary, flower-shaped 3D porous FA-PC sulfur-encapsulating composite cathode materials have been successfully prepared for the first time via a simple thermal treatment process. The FA-PC/S electrodes deliver a higher reversible specific capacity and cycle efficiency compared to PC/S

dx.doi.org/10.1021/sc500459c | ACS Sustainable Chem. Eng. 2014, 2, 2442−2447

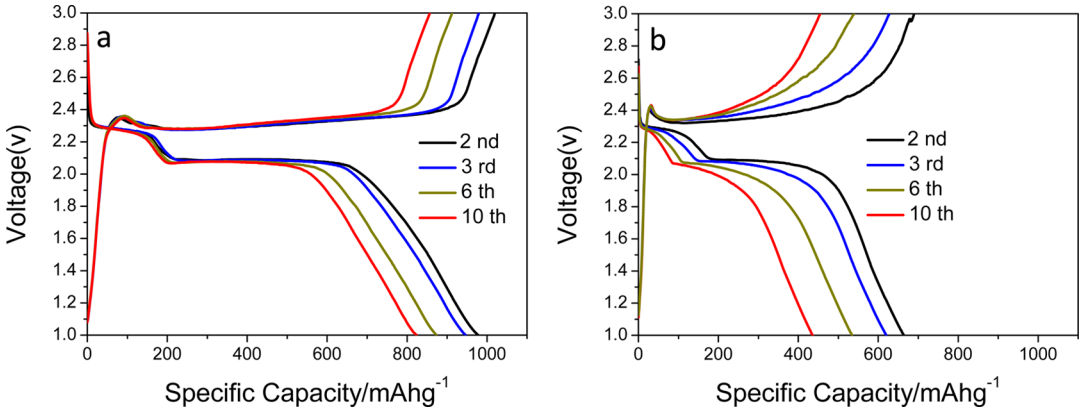

Figure 7. Second, thrid, sixth, and tenth galvanostatic charge−discharge profiles of FA-PC/S (a) and PC/S (b) at 200 mA g^{-1}.

electrodes. These results are attributed to the unique abundant microporous structure of FA-PC, which not only contains enough micropores to store active sulfur but also has enough remaining space to accommodate the volume expansion problem and prevent active sulfur and intermediate products from dissolving in the electrolyte during the discharge process for Li−S batteries. This characteristic contributes to retaining the stability of the FA-PC/S electrode material and the integrity of the electrode before and after discharge. The stable flower-shaped 3D FA-PC/S electrodes exhibit excellent electrochemical properties and are promising candidates for cathode materials for lithium−sulfur cells.

AUTHOR INFORMATION

Corresponding Authors

*Tel.: +86-21-51630320. Fax: +86-21-51630320. E-mail: huangt@fudan.edu.cn (T.H.).

*Tel.: +86-21-51630320. Fax: +86-21-51630320. E-mail: asyu@fudan.edu.cn (A.Y.).

Notes

The authors declare no competing financial interest.

ACKNOWLEDGMENTS

The authors acknowledge funding support from the 973 Program (No. 2013CB934103), National Natural Science Foundation (No. 21173054), and Science & Technology Commission of Shanghai Municipality (No. 08DZ2270500), China.

REFERENCES

(1) Ellis, B. L.; Lee, K. T.; Nazar, L. F. Positive electrode materials for Li ion and Li-batteries. *Chem. Mater.* **2010**, *22*, 691−714.

(2) Chen, H. W.; Dong, W. L.; Ge, J.; Wang, C. H.; Wu, X. D.; Lu, W.; Chen, L. W. Ultrafine sulfur nanoparticles in conducting polymer shell as cathode materials for high performance lithium/sulfur batteries. *Sci. Rep.* **2013**, *3*, 1910−1915.

(3) Bruce, P. G.; Freunberger, S. A.; Hardwick, L. J.; Tarascon, J. M. Li−O_2 and Li−S batteries with high energy storage. *Nat. Mater.* **2012**, *11*, 19−29.

(4) Cao, Y.; Li, X.; Aksay, I. A.; Lemmon, J.; Nie, Z.; Yang, Z.; Liu, J. Sandwich-type functionalized graphene sheet-sulfur nanocomposite for rechargeable lithium batteries. *Phys. Chem. Chem. Phys.* **2011**, *13*, 7660−7665.

(5) Manthiram, A.; Fu, Y.; Su, Y.-S. Challenges and prospects of lithium−sulfur batteries. *Acc. Chem. Res.* **2013**, *4*, 1125−1134.

(6) Ji, X. L.; Nazar, L. F. Advances in Li−S batteries. *J. Mater. Chem.* **2010**, *20*, 9821−9826.

(7) Rauh, R. D.; Abraham, K. M.; Pearson, G. F.; Surprenant, J. K.; Brummer, S. B. A lithium/dissolved sulphur battery with an organic electrolyte. *J. Electrochem. Soc.* **1979**, *126*, 523−527.

(8) Shim, J.; Striebel, K. A.; Cairns, E. J. The lithium/sulfur rechargeable cell. *J. Electrochem. Soc.* **2002**, *149*, A1321−A1325.

(9) Yuan, L. X.; Feng, J. K.; Ai, X. P.; Cao, Y. L.; Chen, S. L.; Yang, H. X. Improved dischargeability and reversibility of sulfur cathode in a novel ionic liquid electrolyte. *Electrochem. Commun.* **2006**, *8*, 610−614.

(10) He, X.; Ren, J.; Wang, L.; Pu, W.; Jiang, C.; Wan, C. Expansion and shrinkage of the sulfur composite electrode in rechargeable lithium batteries. *J. Power Sources* **2009**, *190*, 154−156.

(11) Rauh, R. D.; Shuker, F. S.; Marston, J. M. Formation of lithium polysulfides in aprotic media. *J. Inorg. Nucl. Chem.* **1977**, *39*, 1761−1766.

(12) Ji, X. L.; Lee, K. T.; Nazar, L. F. A highly ordered nanostructured carbon−sulphur cathode for lithium−sulphur batteries. *Nat. Mater.* **2009**, *8*, 500−506.

(13) Li, D.; Han, F.; Wang, S.; Cheng, F.; Sun, Q.; Li, W. C. High sulfur loading cathodes fabricated using peapodlike, large pore volume mesoporous carbon for lithium−sulfur battery. *ACS Appl. Mater. Interfaces* **2013**, *5*, 2208−2213.

(14) Wang, C. H.; Chen, H. W.; Dong, W. L.; Ge, J.; Lu, W.; Wu, X. D.; Guo, L.; Chen, L. W. Sulfur−amine chemistry-based synthesis of multi-walled carbon nanotube−sulfur composites for high performance Li−S batteries. *Chem. Commun.* **2014**, *50*, 1202−1204.

(15) Elazari, R.; Salitra, G.; Garsuch, A.; Panchenko, A.; Aurbach, D. Sulfur-impregnated activated carbon fiber cloth as a binder-free cathode for rechargeable Li−S batteries. *Adv. Mater.* **2011**, *23*, 5641−5644.

(16) Zhou, L.; Lin, X. J.; Huang, T.; Yu, A. S. Binder-free phenyl sulfonated graphene/sulfur electrodes with excellent cyclability for lithium sulfur batteries. *J. Mater. Chem. A* **2014**, *2*, 5117−5123.

(17) Zhang, B.; Lai, C.; Zhou, Z.; Gao, X. P. Preparation and electrochemical properties of sulfur−acetylene black composites as cathode materials. *Electrochim. Acta* **2009**, *54*, 3708−3713.

(18) Cao, Y. L.; Li, X. L.; Aksay, I. A.; Lemmon, J.; Nie, Z. M.; Yang, Z. G. Sandwich-type functionalized graphene sheet-sulfur nanocomposite for rechargeable lithium batteries. *J. Phys. Chem. Chem. Phys.* **2011**, *13*, 7660−7665.

(19) Wang, J. L.; Yang, J.; Xie, J. Y.; Xu, N. X.; Li, Y. Sulfur−carbon nano-composite as cathode for rechargeable lithium battery based on gel electrolyte. *Electrochem. Commun.* **2002**, *4*, 499−502.

(20) Sun, Y. J.; Wang, L.; Yu, X. G.; Chen, K. Z. Facile synthesis of flower-like 3D ZnO superstructures via solution route. *CrystEngComm.* **2012**, *14*, 3199−3204.

(21) Li, B. X.; Wang, Y. F. Facile synthesis and enhanced photocatalytic performance of flower-like ZnO hierarchical microstructures. *J.Phys.Chem.C* **2010**, *114*, 890−896.

(22) Wang, Q.; Yan, J.; Wang, Y. B.; Wei, T.; Zhang, M. L.; Jing, X. Y.; Fan, Z. J. Three-dimensional flower-like and hierarchical porous

carbon materials as high-rate performance electrodes for supercapacitors. *carbon* **2014**, *67*, 119−127.
(23) Yoon, S. H.; Lim, S.; Song, Y.; Ota, Y.; Qiao, W.; Tanaka, A.; Mochida, I. KOH activation of carbon nanofibers. *Carbon* **2004**, *42*, 1723−1729.
(24) Sevilla, M.; Fuertes, A. B. Sustainable porous carbons with a superior performance for CO_2 capture. *Energy Environ. Sci.* **2011**, *4*, 1765−1771.
(25) Zhang, B.; Qin, X.; Li, G. R.; Gao, X. P. Enhancement of long stability of sulfur cathode by encapsulating sulfur into micropores of carbon spheres. *Energy Environ. Sci.* **2010**, *3*, 1531−1537.
(26) Li, J. Y.; Ding, B.; Xu, G. Y.; Hou, L. R.; Zhang, X. G.; Yuan, C. Z. Enhanced cycling performance and electrochemical reversibility of a novel sulfur-impregnated mesoporous hollow TiO_2 sphere cathode for advanced Li−S batteries. *Nanoscale* **2013**, *5*, 5743−5746.
(27) Zhou, L.; Lin, X. J.; Huang, T.; Yu, A. S. Nitrogen-doped porous carbon nanofiber webs/sulfur composites as cathode materials for lithium−sulfur batteries. *Electrochim. Acta* **2014**, *116*, 210−216.
(28) Suo, L. M.; Hu, Y. S.; Li, H.; Armand, M.; Chen, L. Q. A new class of solvent-in-salt electrolyte for high-energy rechargeable metallic lithium batteries. *Nat. Mater.* **2013**, *4*, 1481−1489.
(29) Zhang, Y. Z.; Liu, S.; Li, G. C.; Li, G. R.; Gao, X. P. Sulfur/polyacrylonitrile/carbon multi-composites as cathode materials for lithium/sulfur battery in the concentrated electrolyte. *J. Mater. Chem. A* **2014**, *2*, 4652−4659.
(30) Shin, E. S.; Kim, K.; Oh, S. H.; Cho, W. I. Polysulfide dissolution control: The common ion effect. *Chem. Commun.* **2013**, *49*, 2004−2006.
(31) Jayaprakash, N.; Shen, J.; Moganty, S. S.; Corona, A.; Archer, L. A. Porous hollow carbon@sulfur composites for high-power lithium−sulfur batteries. *Angew. Chem.* **2011**, *123*, 6026−6030.
(32) Zheng, G.; Yang, Y.; Cha, J. J.; Hong, S. S.; Cui, Y. Hollow carbon nanofiber-encapsulated sulfur cathodes for high specific capacity rechargeable lithium batteries. *Nano Lett.* **2011**, *11*, 4462−4467.
(33) Ding, N.; Chien, S. W.; Andy Hor, T. S.; Liu, Z. l.; Zong, Y. Key parameters in design of lithium sulphur batteries. *J. Power Sources* **2014**, *269*, 111−116.
(34) Marmorstein, D.; Yu, T. H.; Striebel, K. A.; McLarnon, F. R.; Hou, J.; Cairns, E. J. Electrochemical performance of lithium/sulfur cells with three different polymer electrolytes. *J. Power Sources* **2000**, *89*, 219−226.
(35) Mikhaylik, Y. V.; Akridge, J. R. Polysulfide shuttle study in the Li/S Battery system. *J. Electrochem. Soc.* **2004**, *151*, A1969−A1976.
(36) Wen, X. R.; Zhang, D. S.; Shi, L. Y.; Yan, T. T.; Wang, H.; Zhang, J. P. Three-dimensional hierarchical porous carbon with a bimodal pore arrangement for capacitive deionization. *J. Mater. Chem.* **2012**, *45*, 23835−23844.
(37) Chen, Z.; Wen, J.; Yan, C.; Rice, L.; Sohn, H.; Shen, M. High-performance supercapacitors based on hierarchically porous graphite particles. *Adv. Energy Mater.* **2011**, *4*, 551−556.